Geochemical Journal, Vol. 41, pp. 29 to 45, 2007

South China provenance of the lower-grade Penglai Group north of the Sulu UHP orogenic belt, eastern China: Evidence from detrital zircon ages and Nd-Hf isotopic composition

XIANG-HUI LI,[1,2] FUKUN CHEN,[1,3]* JING-HUI GUO,[1,3] QIU-LI LI,[1] LIE-WEN XIE[3] and WOLFGANG SIEBEL[4]

[1]Key Laboratory of Mineral Resources, Institute of Geology and Geophysics, Chinese Academy of Sciences, Beijing 100029, China
[2]School of Earth Sciences, Graduate University of Chinese Academy of Sciences, Beijing 100039, China
[3]State Key Laboratory of Lithospheric Evolution, Institute of Geology and Geophysics, Chinese Academy of Sciences, Beijing 100029, China
[4]Institut für Geowissenschaften, Universität Tübingen, 72074 Tübingen, Germany

(*Received January 26, 2006; Accepted September 28, 2006*)

The Dabie-Sulu ultrahigh-pressure orogenic belt resulted from the early Mesozoic collision of the North China block and South China block (comprising the Yangtze and the Cathaysia) and subsequent exhumation of the subducted South China continental slabs. This belt consists of tectonically juxtaposed rock units of different metamorphic grade. Provenance of the low-grade metamorphic terranes exposed along the northern part of the belt can offer useful information about the location of the boundary between these two continental blocks. This study reports detrital zircon ages and Nd-Hf isotopic composition of sedimentary rocks of the low-grade Penglai Group, situated north of the Sulu UHP terrane. Results show that detrital zircon grains mostly crystallized during Mesoproterozoic time, clustering at 1.7 Ga to 1.6 Ga and 1.2 Ga. Nd isotopic composition (T_{DM} value) of the Penglai Group suggests that sedimentary sources are similar to average crustal material of the Yangtze block and mostly formed in Paleo- to Mesoproterozoic. Late Mesoproterozoic detrital zircons probably demonstrate that sedimentary material was derived from the boundary of the Yangtze and Cathaysia blocks, which was formed by the late Mesoproterozoic convergence. Absence of Neoproterozoic detrital zircons from the Penglai sediments probably suggests a late Mesoproterozoic to early Neoproterozoic deposition age (about 1.1 Ga to 0.8 Ga). The age and isotopic evidence implies that the Penglai Group originated from the South China block and probably was thrust onto the basement of the North China block during the early Mesozoic continental collision.

Keywords: Sulu UHP belt, lower-grade, detrital zircon age, Nd-Hf isotopes, provenance

INTRODUCTION

The Dabie-Sulu ultrahigh-pressure (UHP) orogenic belt represents the eastern part of the Qinling-Dabie orogenic belt in central China, which was formed by collision of the North China block and the South China block during the early Mesozoic (e.g., Mattauer *et al.*, 1985; Hsü *et al.*, 1987; Wang *et al.*, 1989; Zhang, G.-W. *et al.*, 1995; Meng and Zhang, 1999, 2000). The latter comprises the Yangtze block in the northwest and the Cathaysia block in the southeast (Fig. 1a). The time of final collision and exhumation of subducted continental slabs has been well constrained to early Mesozoic by numerous radiometric studies (e.g., Ames *et al.*, 1993; Li *et al.*, 1993; Zheng *et al.*, 2002). Typical UHP metamorphic mineral inclusions, such as coesite and diamond, are found in garnet and zircon, indicating deep subduction of continental crust during the collision (e.g., Liou *et al.*, 1996; Xu *et al.*, 1992; Jahn *et al.*, 1996; Li *et al.*, 1999).

Along the northern margin of the Dabie-Sulu UHP orogenic belt, a low-grade metamorphic belt probably related to the UHP metamorphism is exposed. This metamorphic belt is represented by several rock units. They are commonly referred to as the Beihuaiyang low-grade metamorphic zone in the northern foot of the Dabie Mountains, and the Wulian and Penglai Groups in the northern part of the Sulu UHP terrane (Fig. 1; Zheng *et al.*, 2005). Metamorphic grade of these rock units mainly reach greenschist-facies conditions and folding and thrusting are commonly observed (Zhou *et al.*, 2005). Studies on sedimentary sources, provenance, and tectonic setting of these low-grade metamorphic rock units will enhance our understanding of the tectonic boundary between the North China and Yangtze blocks and help to reconstruct the tectonic evolution of the Dabie-Sulu orogenic belt. In recent years, several studies have been made on the

*Corresponding author (e-mail: fukun-chen@mail.igcas.ac.cn)

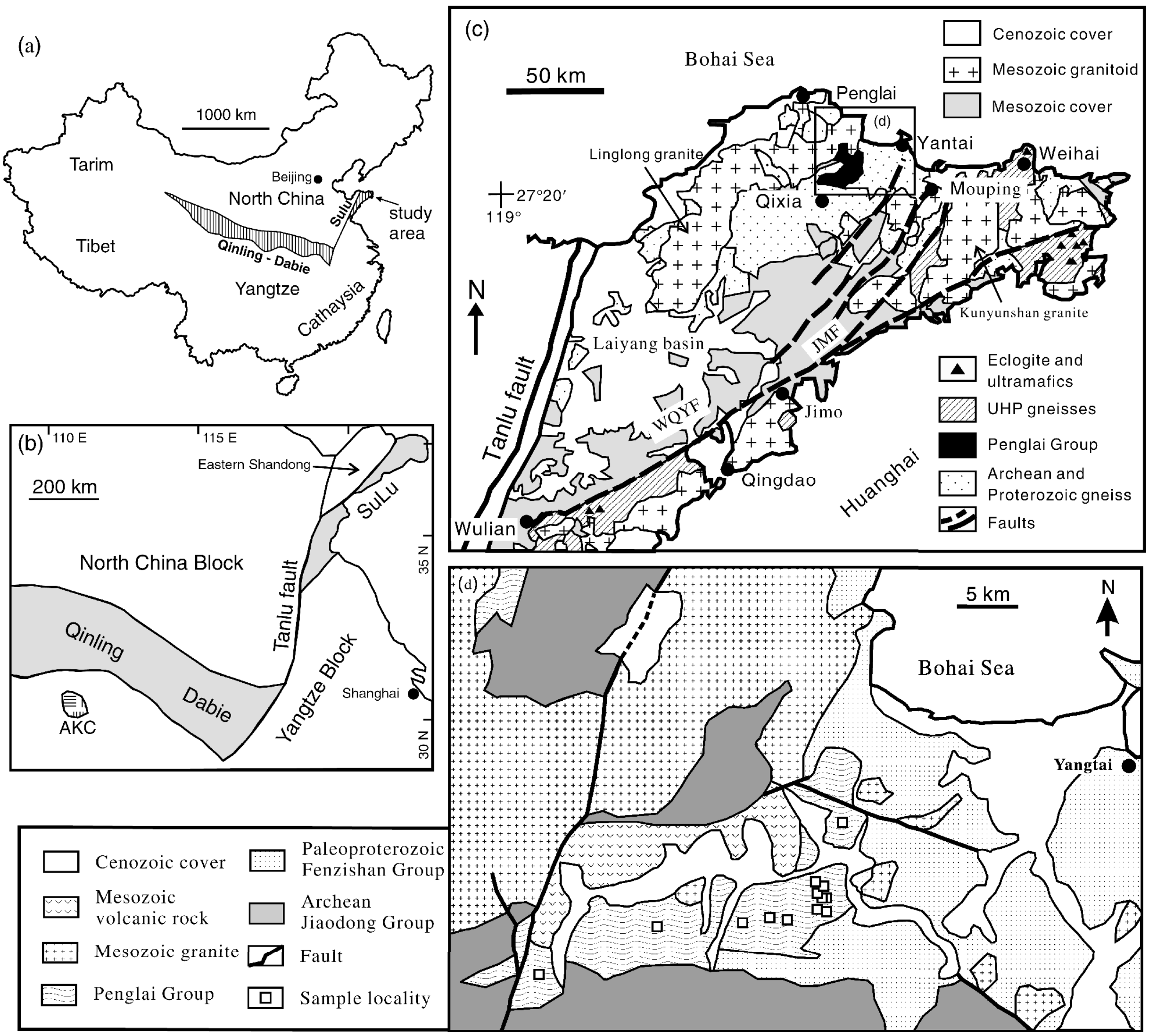

Fig. 1. (a) and (b) Sketch maps showing localities of the major geological units in China and the Qinling-Dabie-Sulu orogenic belt. (c) Simplified geological map of the eastern Shandong Province (or the Jiaodong area) after Guo et al. (2005). (d) Geological map of study area after Zhu et al. (1994), showing the sample localities. Abbreviations: JMF, Jimo-Mouping fault; WQYF: Wulian-Qingdao-Yangtai fault; UHP, ultrahigh-pressure. AKC: the Archean Kongling Complex.

Beihuaiyang low-grade metamorphic zone and the Wulian Group to obtain evidence of the provenance of these terranes (Chen, F. *et al*., 2003; Zheng *et al*., 2005; Wu *et al*., 2004; Zhou *et al*., 2001, 2003, 2005). For discussion of the tectonic setting of these terranes see Chen, F. *et al*. (2003) and Zheng *et al*. (2005). Compared to the Beihuaiyang zone and the Wulian Group, only a few studies have been performed on the Penglai Group. The source and deposition time (i.e., whether late Proterozoic or early Paleozoic) of this group is still a subject of considerable debate (Zhu *et al*., 1994; Ji and Zhao, 1992; Niu *et al*., 1996). This study presents geochemical and Nd isotopic data of whole-rock samples as well as age and Hf isotopic data of detrital zircon grains from the Penglai Group, to further constrain sedimentary sources and deposition time and to discuss the provenance of this group.

Geological Setting

The eastern Shandong Province, geologically known as the Jiaodong block, is composed of two types of Precambrian basement (Fig. 1c). Both basement domains have distinct origins and geological evolution and are separated by the Wulian-Qingdao-Yangtai fault. To the east of this fault, the basement is made up mainly of late Proterozoic granitic gneisses, which experienced a thermal event between *ca*. 0.7 to 0.8 Ga (e.g., Ishizaka *et al*., 1994; Guo *et al*., 2005; Ames *et al*., 1996; Hacker *et al*., 1998). This terrain comprises part of the Sulu UHP belt that was subjected to HP-UHP metamorphism during the early Mesozoic (e.g., Cong, 1996; Zhai *et al*., 2000; Guo *et al*., 2005; Liu *et al*., 2001). It is considered as part of the Yangtze block (e.g., Ames *et al*., 1996; Hacker *et al*., 1998; Guo *et al*., 2005). The basement of the western Jiaodong block is mainly composed of the Archean Jiaodong Complex and the Paleoproterozoic Jingshan and Fenzishan Groups. Traditionally, this basement is considered to be part of the North China block and is made up mainly of Archean tonalite-trondhjemite-granodiorite (TTG) gneisses, amphibolites, and Paleoproterozoic metasedimentary sequences (e.g., Ma and Bai, 1998; Guo *et al*., 2005). These rocks underwent amphibolite- to granulite-facies metamorphism at about 1.8 Ga (e.g., Zhai *et al*., 2000; Zhao, 2001). Recently, zircon ages of Neoproterozoic obtained on impure marbles of the Fenzishan Group were interpreted as evidence for a Yangtze affinity of this group that probably was thrusted onto the Archean basement of the North China block during the Mesozoic collision of these two continental blocks (Tang *et al*., 2006). However, additional age data from other rock types of this group is necessary to confirm the Neoproterozoic age of the Fenzishan Group.

The Sulu UHP belt is a geological counterpart of the Dabie UHP belt. Both terranes are made up of several tectonically juxtaposed zones of different metamorphic facies, characterized by HP and UHP metamorphism (e.g., Cong 1996; Hacker *et al*., 1998). In the Sulu area, UHP metamorphic rocks are exposed in the northern and central parts (Fig. 1c), while HP to upper greenschist-facies metamorphic rocks, e.g. the Zhangbaling Group and the Haizhou Group, are located in the southern part of this belt. In the north, the UHP terrane is tectonically directly juxtaposed with the Archean to Paleoproterozoic gneisses (Fig. 1c), separated by the Wulian-Qingdao-Yangtai fault (WQYF) that is generally considered as the boundary between the Sulu UHP belt and the North China block (e.g., Yin and Nie, 1993; Ishizaka *et al*., 1994; Cong, 1996). To the south, this boundary is covered by Mesozoic sedimentary rocks of the Laiyang basin. Abundant eclogites of UHP metamorphic phase occur as pods or bodies in orthogneisses of TTG and granitic composition of late Proterozoic age (e.g., Ames *et al*., 1996; Ishizaka *et al*., 1994), which were subjected to metamorphism similar to that of the Dabie UHP belt between 240 Ma and 220 Ma (e.g., Wang *et al*., 1993; Li *et al*., 1993). The UHP metamorphic rocks in the Sulu area, especially in the Weihai area, underwent a granulite-facies overprint during the uplift of the UHP terrane (Zhang, R.-Y. *et al*., 1995; Banno *et al*., 2000). Migmatization is usually developed around strongly retrograded UHP blocks (Wang *et al*., 1993; Jahn *et al*., 1996). The UHP terrane is intruded by numerous Mesozoic granitic rocks which formed during different intervals and in different tectonic settings, such as in syn- to post-collisional settings between about 220 Ma to 160 Ma and in an extensional setting probably related to lithospheric thinning or subduction of the paleo-Pacific plate around 120 Ma, after the final collision of the Yangtze and North China blocks (e.g., Guo *et al*., 2005, Wang *et al*., 1998; Yang *et al*., 2005; Chen, J.-F. *et al*., 2003).

North of the Wulian-Qingdao-Yangtai fault (WQYF), low-grade metamorphic rock units are exposed, such as the Wulian Group and the Penglai Group that are markedly different from neighborhood rock units, i.e., the Archean to early Proterozoic high-grade gneisses (Fig. 1). The Penglai Group is composed mainly of slate, schist and quartz sandstone. It forms outcrops northeast of Qixia county and occurs sporadically around Penglai and on small islands north of Yangtai. The sedimentary rocks underwent mainly lower greenschist-facies metamorphism in late Paleozoic and are considered as cover of the Archean to Paleoproterozic basement rocks (e.g., Zhu *et al*., 1994). The deposition age of the Penglai Group was constrained to be Paleozoic by means of Rb-Sr isotopic dating (about 473 Ma) and paleontological methods (e.g., Zhu *et al*., 1994; Ji and Zhao, 1992) and to be late Mesoproterozoic (1166 Ma) by whole-rock Pb-Pb dating (Zhang, 1995). However, due to the mobility of Rb-Sr isotopic systematics during metamorphism, possible inhomogeneous initial Pb isotopic composition of whole-rocks, and problematic dating of paleontological methods, dispute about the time of deposition still remains (Zhu *et al*., 1994; Ji and Zhao, 1992; Niu *et al*., 1996). Further discussion on sedimentary source and provenance of this rock unit requires additional geochemical and isotopic investigation. In this study, fifteen samples comprising schists and quartz sandstones were collected from the Penglai Group north of Qixia (Fig. 1d) for geochemical and Sm-Nd isotopic analyses. Detrital zircon grains were separated from four representative sandstone samples for single grain evaporation $^{207}Pb/^{206}Pb$ dating and Hf isotopic composition.

Analytical Methods

Whole-rock powder was obtained by crushing and splitting of about 10 kg of rock sample. Zircon was isolated from crushed rocks by standard mineral separation techniques and was finally handpicked using a binocular microscope. Zircon grains utilised for cathodoluminescence (CL) study were mounted in epoxy resin and polished down to expose the grain centers. CL images were obtained on a microprobe CAMECA SX51 at the Institute of Geology and Geophysics, Chinese Academy of Sciences (IGG CAS). Zircon Pb-Pb evaporation analysis was performed on a GV IsoProbe-T mass spectrometer and Sm-Nd isotopic ratios were measured on a Finnigan MAT-262 mass spectrometer in the Laboratory for Radiogenic Isotope Geochemistry, IGG CAS.

The principle of the zircon evaporation dating method used in this study is that of Kober (1986, 1987). The analytical technique, however, is different from the conventional procedure. The GV IsoProbe-T mass spectrometer in the Laboratory for Radiogenic Isotope Geochemistry of the IGG CAS is equipped with a multi-ion-counter configuration with seven ion-counters. Intensities of Pb isotopes (^{204}Pb, ^{206}Pb, ^{207}Pb, and ^{208}Pb) extruded from the evaporated zircon grain were statically measured using four ion-counters during evaporation. Pb isotopic ratios were simultaneously measured during the stepwise heating of each zircon, avoiding time-consuming evaporation-deposition cycles employed in the conventional evaporation dating technique. The measurement was terminated with the exhaustion of Pb from the zircon grain and the age value was calculated from those $^{207}Pb/^{206}Pb$ ratios having a constant value. Gain calibration of the different ion-counters was done by measurement on Pb standard solutions (NBS981 and/or NBS982). Common Pb contribution was corrected using values of Stacey and Kramers (1975). Using this technique, variation of the $^{207}Pb/^{206}Pb$ and $^{208}Pb/^{206}Pb$ ratios can be directly observed during the simultaneous evaporation and measurement run. These variations are related to the crystallization history and the distribution of the U and Th content within the zircon grains. More details on analytical techniques are given in Chen *et al*. (2005). During the course of this study, standard zircon grains from Kuehl Lake/Canada (zircon 91500, Wiedenbeck *et al*., 1995) were measured and the results (mean $^{207}Pb/^{206}Pb$ age of 1062 ± 5 Ma) are comparable to the ages derived from isotope dilution analyses (Wiedenbeck *et al*., 1995) and conventional zircon Pb evaporation (Chen *et al*., 2002). Ages obtained by the evaporation method are given as weighted average and errors refer to the 95% confidence level, calculated using the Isoplot program (Ludwig, 2001).

For Sm-Nd isotope analysis, rare earth elements were isolated on quartz columns by conventional ion exchange chromatography with a 5-ml resin bed of AG 50W-X12 (200–400 mesh). Nd and Sm were separated from other rare-earth elements on quartz columns using 1.7-ml Teflon powder coated with HDEHP, di(2-ethylhexyl)orthophosphoric acid, as the cation exchange medium. Sm and Nd were loaded as phosphate on preconditioned Re filaments and measurements were performed in a Re double filament configuration. $^{143}Nd/^{144}Nd$ ratios are normalized to $^{146}Nd/^{144}Nd = 0.7219$. Repeated measurements on the solution of the Ames metal in year 2004/2005 gave a mean value of 0.512149 ± 0.000022 (2σ, $n = 98$) for the $^{143}Nd/^{144}Nd$ ratio in the Laboratory for Radiogenic Isotope Geochemistry of the IGG CAS (Chen *et al*., 2006). The external precision is a 2σ uncertainty based on replicate measurements on these standard solutions over one year. Results of repeated Sm-Nd analyses on the standard material BCR-1 (basalt powder) are also given in Chen *et al*. (2006). For technical details on Sm-Nd analysis the reader is referred to Chen *et al*. (2000). Total procedural blanks were <100 pg for Sm and Nd.

The notations of ε_{Nd}, $f_{(Sm/Nd)}$, T_{DM} are defined following DePaolo *et al*. (1991):

$$\varepsilon_{Nd} = [(^{143}Nd/^{144}Nd)_S/(^{143}Nd/^{144}Nd)_{CHUR} - 1] \times 10000$$

$$f_{(Sm/Nd)} = (^{147}Sm/^{144}Nd)_S/(^{147}Sm/^{144}Nd)_{CHUR} - 1$$

$$T_{DM} = 1/\lambda_{Sm}\ln[1 + (^{143}Nd/^{144}Nd)_S - 0.51315] \\ /[(^{147}Sm/^{144}Nd)_S - 0.2137]$$

where s = sample, $(^{143}Nd/^{144}Nd)_{CHUR} = 0.512638$, and $(^{147}Sm/^{144}Nd)_{CHUR} = 0.1967$.

In-situ zircon Hf isotopic composition was measured on a Finnigan Neptune Multi-Collector ICP-MS, equipped with a 193 nm Geolas laser sampling system, in the MC-ICP-MS laboratory of the IGG CAS. Zircon grains from the CL sample mounts were analyzed, using the CL images for guidance. Analytical spots were 32 μm in diameter and pure Ar gas was used as sample carrier. More details on the analytical procedures and parameters for interference correction are given in Xu *et al*. (2004). Standard zircon (zircon 91500) was used for calibration during the measurement. Isobaric interference of ^{176}Lu on ^{176}Hf was corrected using the intensity of the interference-free ^{175}Lu isotope and a recommended $^{176}Lu/^{175}Lu$ ratio of 0.02655 (Machado and Simonetti, 2001), while isobaric interference of ^{176}Yb on ^{176}Hf isotope was corrected using the interference-free ^{172}Yb isotope and a recommended $^{176}Yb/^{172}Yb$ ratio of 0.5886 (Chu *et al*., 2002). Zircon 91500 was used as the reference standard during routine analyses, with a recommended $^{176}Hf/^{177}Hf$ ratio of 0.282293 ± 28 (Woodhead *et al*., 2004). Statistical data treatment was performed with the ISOPLOT program (Ludwig, 2001). Chondrite data from Blichert-Toft and Albarede (1998) were used for calculation of the $\varepsilon_{Hf}(t)$ values. Depleted mantle model ages (T_{DM}(Hf)) were calculated following Griffin *et al*. (2000).

Geochemical and Nd Isotopic Data

Fourteen samples were analyzed for major element concentrations and seven representative samples were measured for trace element concentrations including the rare earth elements (REE). Analytical data are given in

Table 1. Contents of major and trace elements of metasediments from the Penglai Group

Sample	PL1	PL2	PL3	PL4	PL5	PL6	PL7	PL8	PL9	PL10	PL11	PL12	PL13	PL14
SiO_2	96.39	98.26	79.88	76.80	74.82	96.06	97.39	96.57	71.75	96.96	69.15	50.22	44.02	97.42
TiO_2	0.05	0.04	0.55	0.71	0.60	0.05	0.05	0.09	0.85	0.04	0.91	0.68	0.68	0.05
Al_2O_3	2.08	0.90	9.84	11.62	11.01	1.53	1.22	2.49	13.83	1.64	14.97	12.14	11.38	1.26
Fe_2O_3	0.43	0.00	3.20	2.89	5.69	0.28	0.16	0.08	3.82	0.27	5.23	4.92	4.91	0.00
MnO	0.001	0.000	0.002	0.001	0.008	0.001	0.000	0.002	0.034	0.001	0.037	0.049	0.084	0.000
MgO	0.16	0.11	0.63	0.83	1.05	0.17	0.13	0.18	1.25	0.16	1.08	1.56	2.47	0.14
CaO	0.02	0.02	0.03	0.02	0.03	0.02	0.02	0.02	0.12	0.02	0.04	12.96	15.91	0.02
Na_2O	0.03	0.04	0.07	0.06	0.06	0.49	0.05	0.03	0.08	0.04	0.08	0.75	1.39	0.03
K_2O	0.41	0.16	3.33	3.73	3.63	0.49	0.25	0.44	4.52	0.54	4.95	3.19	2.62	0.35
P_2O_5	0.015	0.004	0.052	0.032	0.096	0.013	0.010	0.015	0.121	0.012	0.076	0.078	0.088	0.008
LOI	0.63	0.28	2.02	2.52	3.08	0.38	0.40	0.72	3.22	0.38	3.33	13.10	16.18	0.27
Total	100.22	99.82	99.60	99.21	100.07	99.49	99.68	100.64	99.60	100.06	99.85	99.64	99.73	99.54
Ba	76.17		389.92				50.77		686.01	76.43	897.02			45.30
Cs	1.012		7.197				0.708		6.566	1.336	3.507			0.914
Nb	6.16		28.13				6.21		38.32	7.36	33.52			6.53
Rb	15.21		135.82				9.39		204.15	19.26	153.37			13.57
Sr	46.45		118.67				12.64		118.98	30.50	102.65			18.51
Y	4.70		22.51				3.89		35.03	3.84	26.97			6.66
Zr	130.01		183.13				213.36		341.72	54.04	296.01			63.28
Hf	3.75		5.85				5.97		10.80	1.67	9.33			1.98
Pb	5.98		8.40				9.55		27.92	5.16	4.19			1.43
Th	1.95		10.16				1.82		17.89	1.75	19.17			1.92
U	0.47		1.60				0.54		3.05	0.33	3.51			0.54
La	7.63		31.80				7.16		43.37	9.04	36.16			7.50
Ce	15.68		64.35				15.12		91.79	19.38	80.28			12.66
Pr	1.78		7.77				1.75		10.56	2.11	9.27			1.83
Nd	6.16		28.13				6.21		38.31	7.36	33.52			6.53
Sm	1.28		5.32				1.24		7.65	1.39	6.84			1.33
Eu	0.21		1.06				0.17		1.47	0.20	1.46			0.20
Gd	1.15		4.39				1.01		6.52	1.07	5.87			1.28
Tb	0.19		0.76				0.16		1.16	0.17	1.01			0.23
Dy	0.94		4.21				0.77		6.53	0.80	5.41			1.27
Ho	0.19		0.85				0.16		1.31	0.16	1.07			0.26
Er	0.57		2.48				0.53		3.81	0.50	3.12			0.79
Tm	0.10		0.39				0.09		0.60	0.08	0.50			0.12
Yb	0.64		2.57				0.65		3.89	0.52	3.33			0.78
Lu	0.10		0.39				0.10		0.60	0.07	0.51			0.11
A/CNK	3.93	3.27	2.61	2.78	2.69	1.11	3.13	4.43	2.63	2.37	2.69	0.43	0.33	2.69
$(La/Yb)_N$	8.51		8.88				7.93		8.00	12.55	7.78			6.93
$(Tb/Yb)_N$	1.33		1.35				1.13		1.36	1.52	1.38			1.34
Eu/Eu*	0.54		0.67				0.45		0.63	0.51	0.70			0.47

Contents of major and trace elements in wt.% and in ppm, respectively.
A/CNK: Mole $Al_2O_3/(CaO + Na_2O + K_2O)$ ratio.
Eu/Eu: $(Eu)_N/((Sm)_N*(Gd)_N)^{1/2}$.*

Table 1. Seven sandstone samples containing predominantly quartz, have SiO_2-contents between 96.06 wt.% and 98.26 wt.%. Five samples of schist (samples PL3, PL4, PL5, PL9 and PL11) containing abundant quartz and feldspar with minor mica have SiO_2 ranging from 69.15 wt.% to 79.88 wt.% and Al_2O_3 from 9.84 wt.% to 14.97 wt.%. Two additional schist samples (samples PL12 and PL13) containing quartz, feldspar and larger amounts of calcite are characterized by high CaO-contents (12.96 and 15.91 wt.%) and high loss of ignition (LOI) of up to 13.10 and 16.18 wt.%.

Normalized trace element and REE compositions of seven samples are plotted in Fig. 2. Compared to the schist samples, the sandstone samples have low contents of trace elements and REEs. Total REE contents of the investigated schist samples (PL3, PL9 and PL11) range from 569 ppm to 806 ppm, while the sandstone samples (PL1, PL7, PL10, PL14) have total REE contents between 127 ppm and 148 ppm. This difference must be caused by different trace element and REE contents of the mineral phases. Sandstone and schist samples have very similar normalized REE and trace element patterns (Figs. 2a and b). Except for Ta-content, analyzed samples of both rock types similarly show depletion in Sr-, Zr-, and Y-contents and enrichment in Pb-content. As seen from the normalized REE patterns, both sandstone and schist samples show fractionation between light and heavy REE and a significant Eu depletion is present in all samples. Both rock types have similar La_N/Yb_N and Tb_N/Yb_N ratios, ranging from 6.93 to 12.55 and 1.13 to 1.52, respectively.

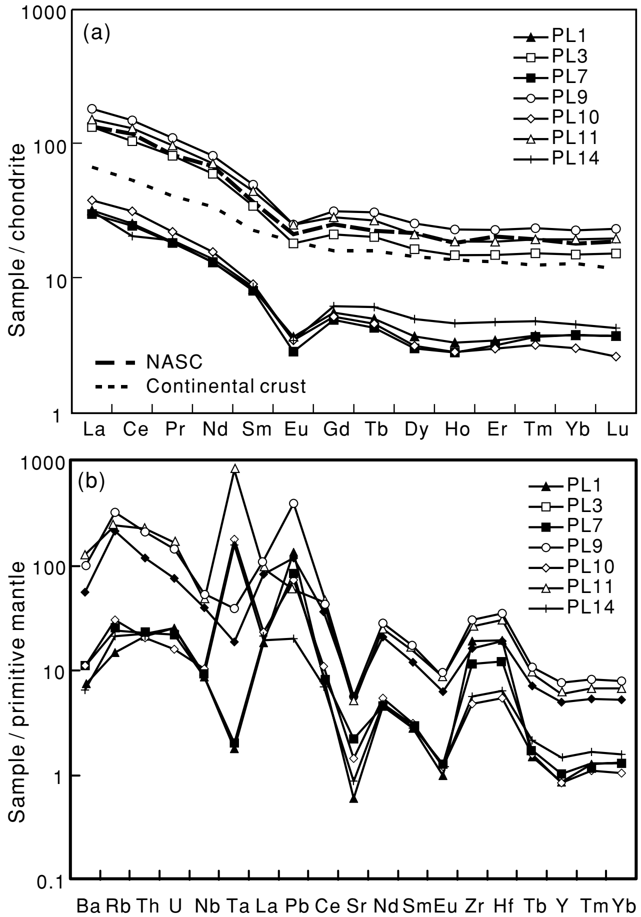

Fig. 2. Normalized rare earth and trace element concentrations of sedimentary rocks. Normalizing values for chondrite and primordial mantle are from Sun (1982) and Taylor and McLennan (1985). Data of the NASC are from Gromet et al. (1984).

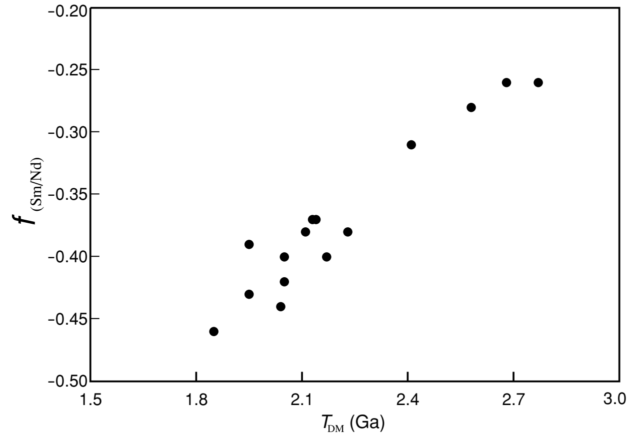

Fig. 3. T_{DM}(Nd) value vs. $f_{(Sm/Nd)}$ value diagram of whole-rock samples of the Penglai sedimentary rocks, showing a positive correlation.

Sandstone samples have slightly lower Eu/Eu* values (0.45 to 0.54) than schist samples (0.63 to 0.70), probably owing to lower feldspar content or different source characteristics. The schist samples of the Penglai Group have similar normalized REE patterns compared to the North American shale composite (NASC (Gromet *et al*., 1984; Fig. 2), but differ from average crustal composition (Taylor and McLennan, 1985) by their higher REE content. It is commonly accepted that fractionation between the REEs is insignificant during sedimentation and low-grade metamorphism (e.g., Taylor and McLennan, 1985). Therefore, the REE patterns of the schist samples from the Penglai Group that have features of post-Archean schists are representative of the REE source characteristic.

Whole-rock Sm-Nd analytical data of fifteen samples of schist and sandstone from the Penglai Group are given in Table 2. Measured $^{143}Nd/^{144}Nd$ ratios of the samples range from 0.511768 to 0.511955. Their Sm/Nd ratios are similar to that of mean continental crust, indicated by $f_{(Sm/Nd)}$ values ranging from –0.46 to –0.26. Using a single-stage model (DePaolo *et al*., 1991), the samples give depleted-mantle model ages (T_{DM}(Nd) values) ranging from 1.85 Ga to 2.77 Ga, clustering around 1.8 Ga to 2.0 Ga (Table 2). The T_{DM}(Nd) values are positively correlated with $f_{(Sm/Nd)}$ values (Fig. 3), implying possible overestimate of the model age values for the samples having high fractionation between Sm and Nd when using the one-stage model. When a two-stage model (Liew and Hofmann, 1988) is used, T_{DM}(Nd) values range tightly from 2.34 Ga to 1.94 Ga (Table 2), indicating a Paleoproterozoic mean crustal residence age for the major sedimentary source(s) of the Penglai Group.

Detrital Zircon Ages and Hf Isotopic Composition

Four representative sandstone samples collected from the Penglai Group contain abundant detrital zircon grains. Most of the grains are well rounded or oval in shape, indicating long-distance transportation and heavy ablation before deposition, being consistent with typical characteristics of detrital zircon grains. Under a binocular microscope, zircon grains appear transparent, light yellow in color, or partly light brown to colorless. Cathodoluminescence (CL) images of zircon grains offer the opportunity to study their internal structure which yields important information about the crystallization history of the grains (e.g., Hanchar and Miller, 1993; Pidgeon *et al*., 1998). Figure 4 shows CL images for typical zircon populations. Most of the grains exhibit oscillatory zoning of magmatic origin, almost lacking

Table 2. Analytical data of whole-rock Sm-Nd isotopic composition

Sample	Sm (ppm)	Nd (ppm)	^{147}Sm/^{144}Nd	^{143}Nd/^{144}Nd	error 2σ	^{143}Nd/^{144}Nd(t) (1.2 Ga)	ε_{Nd}(t) (1.2 Ga)	T_{DM} (Ga)	T_{DM2} (Ga)	$f_{(Sm/Nd)}$
PL1	1.067	5.216	0.1238	0.511882	±11	0.510907	–3.6	2.14	2.10	–0.37
PL2	0.705	3.493	0.1222	0.511879	±13	0.510916	–3.4	2.11	2.09	–0.38
PL3	6.911	39.40	0.1062	0.511843	±12	0.511006	–1.6	1.85	1.94	–0.46
PL4	6.265	30.96	0.1225	0.511809	±11	0.510844	–4.8	2.23	2.20	–0.38
PL5	4.337	21.24	0.1236	0.511886	±10	0.510912	–3.5	2.13	2.10	–0.37
PL6	1.154	6.140	0.1138	0.511799	±10	0.510902	–3.6	2.05	2.11	–0.42
PL7	1.108	5.649	0.1188	0.511866	±10	0.510930	–3.1	2.05	2.07	–0.40
PL8	1.735	9.474	0.1109	0.511768	±10	0.510894	–3.8	2.04	2.12	–0.44
PL9a	3.224	13.40	0.1456	0.511907	±10	0.510760	–6.4	2.77	2.34	–0.26
PL9	11.23	47.66	0.1426	0.511938	±10	0.510815	–5.3	2.58	2.25	–0.28
PL10	1.238	6.644	0.1128	0.511857	±9	0.510969	–2.3	1.95	2.00	–0.43
PL11	4.754	19.89	0.1447	0.511930	±13	0.510790	–5.8	2.68	2.29	–0.26
PL12	4.019	20.66	0.1178	0.511777	±11	0.510849	–4.7	2.17	2.20	–0.40
PL13	3.027	13.58	0.1350	0.511900	±11	0.510836	–4.9	2.41	2.22	–0.31
PL14	1.132	5.673	0.1208	0.511955	±10	0.511003	–1.7	1.95	1.95	–0.39

T_{DM2} values are two-stage model ages using t = 1200 Ma (following Liew and Hofmann, 1988).

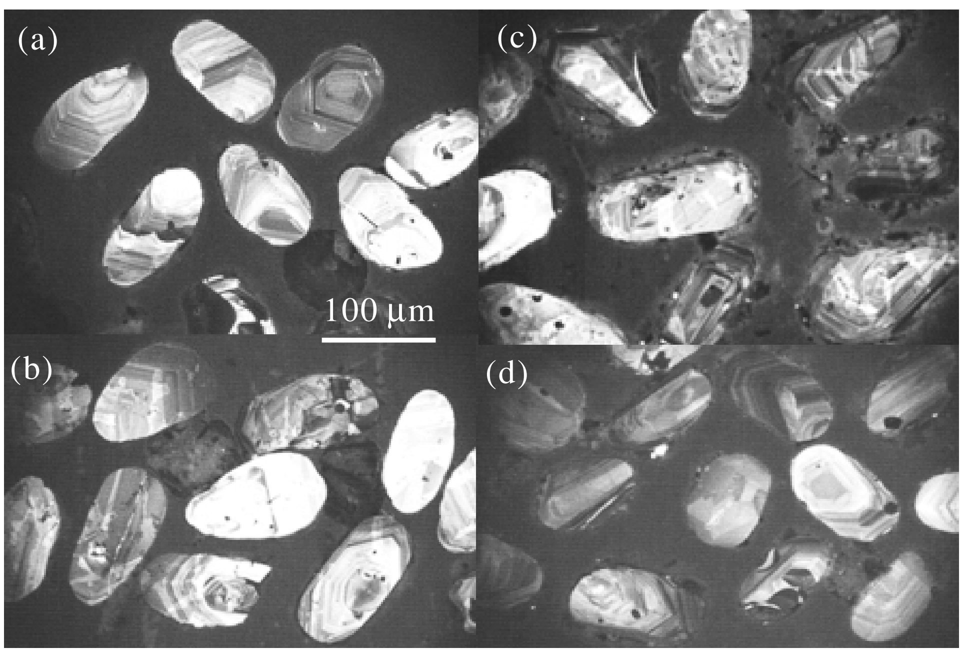

Fig. 4. Cathodoluminescence photographs of typical populations of detrital zircon grains from samples PL1 (a), PL7 (b), PL10 (c), and PL14 (d). Zircon grains are rounded or oval in shape, but magmatic oscillatory zoning is still well preserved, indicating simple histories for most of the grains.

recrystallization phenomena, which suggests a simple post-crystallization history. A small amount of zircon grains without magmatic oscillatory CL zoning are completely recrystallized, implying an overprint by later metamorphic events. A minority of zircon grains contain inherited cores, for instance the two grains in the lower part of Fig. 4b. It is clearly shown in the CL images that most of the detrital zircon grains were mechanically rounded during transportation of the sedimentary material.

Zircon grains from three sandstone samples were evaporated for Pb isotope composition and the analytical data are given in Table 3. ^{207}Pb/^{206}Pb ratios of 51 evaporated zircon grains correspond to ages that range from 2514 ± 5 Ma to 1087 ± 9 Ma. The distribution of the ^{207}Pb/

Table 3. Single zircon evaporation Pb-Pb data of metasediments from the Penglai Group

Grain No.	Number of scan	$^{207}Pb^*/^{206}Pb^*$	Age (Ma) (2σ)	$^{208}Pb^*/^{206}Pb^*$	Th/U
PL1					
1	70	0.09902	1606 ± 7	0.0746	0.25
2	60	0.08165	1237 ± 24	0.2323	0.78
3	67	0.10060	1635 ± 24	0.2625	0.88
4	81	0.09350	1498 ± 23	0.1802	0.60
5	120	0.08038	1206 ± 13	0.2522	0.84
6	46	0.08980	1421 ± 29	0.3130	1.05
7	170	0.07905	1173 ± 7	0.1290	0.43
8	120	0.10093	1641 ± 9	0.2337	0.78
9	178	0.09449	1518 ± 7	0.0748	0.25
10	83	0.10940	1789 ± 18	0.0836	0.28
11	60	0.10283	1676 ± 16	0.2339	0.78
12	121	0.09744	1575 ± 11	0.0200	0.07
13	90	0.16561	2514 ± 5	0.0742	0.25
14	59	0.10070	1637 ± 11	0.2670	0.89
15	44	0.08313	1272 ± 19	0.1852	0.62
16	36	0.09935	1613 ± 10	0.5151	1.72
17	40	0.08380	1288 ± 21	0.2569	0.86
PL7					
1	120	0.10048	1633 ± 9	0.1559	0.52
2	60	0.10108	1644 ± 9	0.1487	0.50
3	58	0.10130	1648 ± 20	0.2285	0.76
4	108	0.10259	1672 ± 18	0.2099	0.70
5	60	0.09281	1484 ± 9	0.0922	0.31
6	119	0.10687	1747 ± 7	0.1637	0.55
7	119	0.09617	1551 ± 12	0.1812	0.61
8	120	0.07907	1174 ± 17	0.2795	0.93
9	45	0.09100	1447 ± 27	0.2076	0.69
10	105	0.08010	1200 ± 15	0.2272	0.76
11	113	0.07788	1144 ± 8	0.2599	0.87
12	75	0.10536	1721 ± 11	0.1581	0.53
13	41	0.10064	1636 ± 14	0.2005	0.67
14	54	0.09690	1565 ± 24	0.2377	0.80
15	113	0.08863	1396 ± 7	0.2030	0.68
16	52	0.10399	1697 ± 15	0.1270	0.42
17	57	0.09212	1470 ± 9	0.1408	0.47
18	53	0.07654	1108 ± 11	0.0857	0.29
19	56	0.08842	1391 ± 15	0.0590	0.20
PL10					
1	77	0.08478	1311 ± 19	0.4349	1.45
2	137	0.09827	1592 ± 9	0.1078	0.36
3	50	0.13400	2151 ± 21	0.0838	0.28
4	164	0.07574	1087 ± 9	0.6370	2.13
5	119	0.10960	1793 ± 5	0.0434	0.15
6	45	0.08032	1204 ± 15	0.3887	1.30
7	73	0.08070	1214 ± 12	0.3818	1.28
8	176	0.10324	1683 ± 8	0.1494	0.50
9	102	0.10206	1663 ± 15	0.1978	0.66
10	60	0.07930	1180 ± 30	0.2570	0.86
11	75	0.08037	1207 ± 22	0.2337	0.78
12	110	0.10202	1661 ± 11	0.2044	0.68
13	73	0.10368	1691 ± 17	0.2620	0.88
14	180	0.10649	1740 ± 13	0.1517	0.51
15	84	0.10073	1637 ± 9	0.1378	0.46

Th/U ratios are calculated at 1.2 Ga.

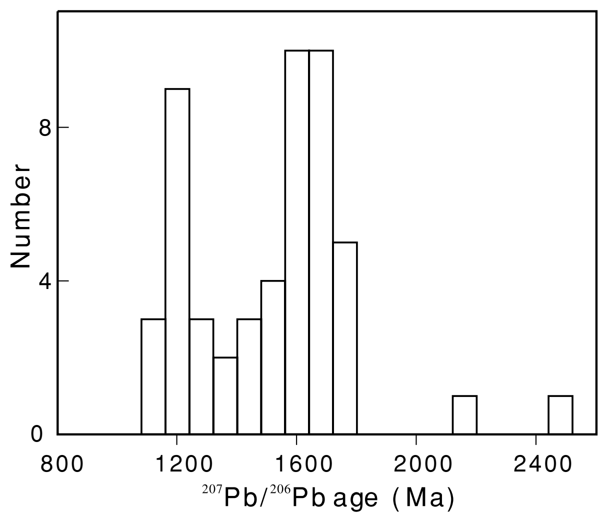

Fig. 5. Frequency histogram of zircon ages of samples PL1, PL7 and PL10, obtained by the Pb evaporation method. The age values cluster around 1.7–1.6 Ga and 1.2 Ga.

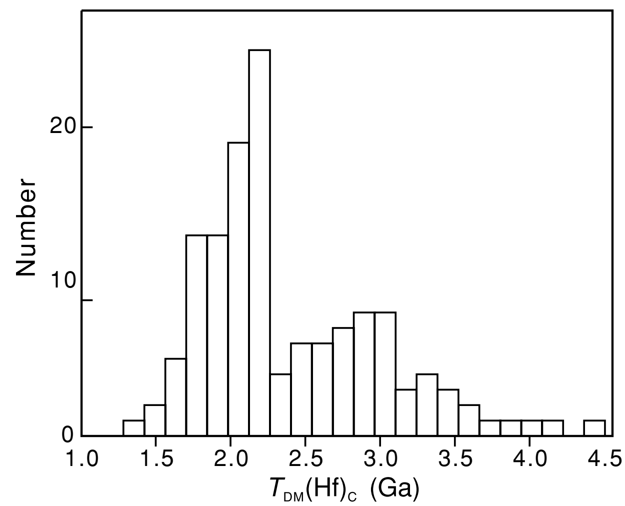

Fig. 6. Frequency histogram of T_{DM}(Hf) values of zircon grains of samples PL1, PL7, PL10 and PL14, obtained by the in-situ LA-MC-ICP-MS method. T_{DM}(Hf) values calculated using crustal Lu/Hf ratios (Veevers et al., 2005), giving two age peaks around 2.2–2.0 Ga and 3.0 Ga.

^{206}Pb ages is shown in a histogram (Fig. 5). Most of zircon grains give ages between 1.8–1.1 Ga clustering around 1.7–1.6 Ga and 1.2 Ga. Only two zircon grains gave ages older than 1.8 Ga. About eighty percent of zircon grains give ^{208}Pb/^{206}Pb ratios higher than 0.1, corresponding to high Th/U ratios when calculated back to 1.2 Ga, indicating a possible magmatic source (e.g., Hoskin and Black, 2000; Rubatto, 2002; Rino *et al*., 2004). This can be also supported by oscillatory magmatic zoning of most zircon grains in the CL images. Therefore, the age distribution of detrital zircon grains from the analyzed samples probably implies that the sedimentary material of the Penglai Group mainly originated from the terranes where Mesoproterozoic magmatic and/or metamorphic rocks were commonly distributed.

A total of 134 zircon grains from four sandstone samples were analyzed for Hf isotopic composition using the LA-MC-ICP MS method. Analytical data are given in Table 4. All zircon grains have low ^{176}Lu/^{177}Hf ratios, but measured ^{176}Hf/^{177}Hf ratios vary widely from 0.28096 to 0.28236 and ε_{Hf} values range from –64.0 to –16.6. When recalculated to 1.2 Ga, about one third of the analyzed zircon grains have positive initial ε_{Hf} values, implying that some of them probably crystallized around 1.2 Ga from magmas having interaction with mantle material. Depleted-mantle model ages given in Table 4 are calculated using ^{176}Lu/^{177}Hf ratios of zircon grains (T_{DM}(Hf)) and a mean crustal ^{176}Lu/^{177}Hf ratio of 0.015 (T_{DM}(Hf)$_C$), following Griffin *et al*. (2000). Distribution of T_{DM}(Hf) and T_{DM}(Hf)$_C$ values are shown in Fig. 6. The T_{DM}(Hf) values range from about 3.2 Ga to 1.2 Ga, with model age accumulations between 1.7 to 1.6 Ga and 2.3 to 2.2 Ga. As zircon normally has low Lu/Hf ratios that can not represent source characteristic, T_{DM}(Hf)$_C$ values better constrain source information. The T_{DM}(Hf)$_C$ values, calculated using 1.2 Ga and the mean crustal ^{176}Lu/^{177}Hf ratio, vary widely from 4.4 Ga to 1.4 Ga, clustering mostly between 2.2 to 2.0 Ga and 2.7 to 3.0 Ga (there seems to be a second cluster in this range), probably implying Paleoproterozoic and Archean (as secondary) crustal material as a major sedimentary source (Iizuka *et al*., 2005).

DISCUSSION

Provenance of the Penglai Group

The location of the boundary between the North China block and the Yangtze (or the South China) block in the Sulu UHP belt is still debated (e.g., Yin and Nie, 1993; Ishizaka *et al*., 1994; Cong, 1996; Zhai *et al*., 2000; Faure *et al*., 2001). In earlier articles it was commonly assumed that the boundary is located along the Jimo-Moping fault (Yin and Nie, 1993; Ishizaka *et al*., 1994; Cong, 1996). Zhai *et al*. (2000) suggested that the high-grade gneiss terrane in the Jiaodong area (eastern Shandong Province) indeed belongs to the North China block and that the boundary is located roughly in the Kunyushan granite batholith, west of the UHP metamorphic rocks. Faure *et al*. (2001) proposed that the gneiss terrane represents a migmatite dome related to the UHP metamorphism and is part of the Dabie-Sulu UHP orogenic belt. According to these authors, the boundary should be located further north in Bohai bay. The low-grade metamorphic Penglai

Table 4. Analytical data of zircon Hf isotopic composition

Analytical spot	$^{176}Lu/^{177}Hf$	$^{176}Hf/^{177}Hf$	Error 2σ	$\varepsilon_{Hf}(0)$	$\varepsilon_{Hf}(t)$ 1.2 Ga	$T_{DM}(Hf)$ (Ma)	$T_{DM}(Hf)_C$ (Ma)
PL1-1	0.001124	0.282000	29	–27.3	–1.60	1769	2123
-2	0.000686	0.282029	26	–26.3	–0.22	1708	2035
-3	0.001044	0.281716	25	–37.4	–11.62	2158	2756
-4	0.000551	0.282027	36	–26.3	–0.19	1705	2033
-5	0.000392	0.281440	37	–47.1	–20.89	2495	3334
-6	0.000499	0.281615	26	–40.9	–14.75	2265	2952
-7	0.000875	0.281998	36	–27.4	–1.47	1760	2115
-8	0.000822	0.281996	41	–27.5	–1.52	1761	2118
-9	0.000820	0.281941	36	–29.4	–3.45	1836	2240
-10	0.001788	0.281857	40	–32.4	–7.20	2002	2478
-11	0.000544	0.281934	39	–29.6	–3.46	1832	2241
-12	0.000452	0.281442	22	–47.0	–20.87	2496	3333
-13	0.000607	0.281833	41	–33.2	–7.12	1974	2472
-14	0.000882	0.281857	44	–32.4	–6.49	1955	2433
-15	0.001392	0.281937	39	–29.5	–4.07	1870	2279
-16	0.000609	0.281569	33	–42.5	–16.46	2333	3059
-17	0.001195	0.281914	44	–30.3	–4.70	1891	2319
-18	0.000367	0.281731	39	–36.8	–10.53	2100	2687
-19	0.001450	0.282304	46	–16.6	8.90	1356	1452
-20	0.000783	0.282173	46	–21.2	4.79	1514	1716
-21	0.000629	0.281796	33	–34.5	–8.44	2025	2556
-22	0.000442	0.281981	41	–28.0	–1.72	1763	2131
-23	0.000703	0.282116	39	–23.2	2.85	1589	1840
-24	0.000945	0.282048	53	–25.6	0.23	1694	2006
-25	0.000958	0.281963	50	–28.6	–2.79	1812	2198
-26	0.000550	0.282187	46	–20.7	5.48	1485	1671
-27	0.000895	0.281692	51	–38.2	–12.34	2182	2801
-28	0.000829	0.282043	42	–25.8	0.14	1696	2012
-29	0.001146	0.282049	23	–25.6	0.10	1702	2015
-30	0.001006	0.281484	22	–45.6	–19.82	2475	3268
-31	0.000942	0.281743	20	–36.4	–10.58	2115	2690
-32	0.001181	0.281810	21	–34.0	–8.38	2035	2552
-33	0.000335	0.281686	20	–38.4	–12.11	2159	2786
-34	0.001445	0.281771	23	–35.4	–9.97	2104	2652
-35	0.000883	0.281588	26	–41.9	–16.02	2324	3031
-36	0.001064	0.281681	21	–38.6	–12.87	2208	2834

Group is exposed within the high-grade gneiss terrane. The provenance and evolution history of this group can therefore be useful for understanding the relationship between the Sulu UHP metamorphic belt of Yangtze-affinity and the high-grade gneiss terrane, which is generally interpreted as part of the North China block.

Detrital zircon ages have been widely used to study growth and reworking of continental crust, provenances of geologic terrains, depositional ages, and sources of sediments (e.g., Rino *et al*., 2004; Iizuka *et al*., 2005; Nelson, 2001; Valverde *et al*., 2000; Chen, F. *et al*., 2003). Principles of this application are based on physical and isotopic characteristics of zircons and the history of different geological terranes (e.g., Valverde *et al*., 2000). The basements of the North China and South China (Yangtze and Cathaysia) blocks are characterized by very different thermo-magmatic histories before they collided in early Mesozoic times (e.g., Yang *et al*., 1986; Ma and Bai, 1998). The South China block is composed of the Yangtze and Cathaysia blocks that amalgamated together in late Mesoproterozoic (e.g., Chen *et al*., 1991; Li *et al*., 1994, 2002). The North China block is typically characterized by Archean to Paleoproterozoic basement rocks, which mainly underwent four major orogenic cycles during 3.0 to 2.9 Ga, 2.6 to 2.5 Ga, 2.4 to 2.3 Ga, and 1.8 to 1.7 Ga. Although small Archean to Paleoproterozoic basement outcrops are exposed along the northwestern and western margins of the Yangtze block (e.g., Qiu *et al*., 2000; Gao *et al*., 2001) and in the northern part of the Cathaysia block (e.g., Li *et al*., 2002; Zhao and Cawood, 1999), both blocks are characterized mostly by younger basement domains of Meso- to Neoproterozoic age that became stable in late Proterozoic and were subjected to major thermal-magmatic events during 1.1 Ga to 1.0 Ga

Table 4. (continued)

Analytical spot	^{176}Lu/^{177}Hf	^{176}Hf/^{177}Hf	Error 2σ	$\varepsilon_{Hf}(0)$	$\varepsilon_{Hf}(t)$ 1.2 Ga	T_{DM}(Hf) (Ma)	T_{DM}(Hf)$_C$ (Ma)
PL7-1	0.000885	0.281720	24	–37.2	–11.35	2144	2739
-2	0.000984	0.282049	23	–25.6	0.23	1695	2006
-3	0.001219	0.281792	22	–34.7	–9.05	2062	2594
-4	0.000789	0.281957	20	–28.8	–2.85	1812	2202
-5	0.000693	0.282172	24	–21.2	4.85	1511	1711
-6	0.000655	0.281656	25	–39.5	–13.43	2218	2869
-7	0.000749	0.282004	19	–27.2	–1.16	1746	2095
-8	0.002316	0.282223	21	–19.4	5.33	1505	1681
-9	0.001796	0.282365	46	–14.4	10.80	1281	1329
-10	0.000885	0.282212	36	–19.8	6.11	1463	1631
-11	0.000620	0.282219	24	–19.5	6.57	1443	1601
-12	0.000558	0.282118	36	–23.1	3.03	1581	1828
-13	0.000244	0.281536	42	–43.7	–17.36	2357	3115
-14	0.001633	0.282112	32	–23.4	1.94	1635	1897
-15	0.001079	0.281948	44	–29.1	–3.42	1839	2238
-16	0.001622	0.281428	36	–47.5	–22.27	2592	3420
-17	0.000580	0.281992	35	–27.6	–1.46	1755	2114
-18	0.000238	0.281500	34	–45.0	–18.64	2405	3194
-19	0.001123	0.282078	36	–24.5	1.16	1660	1947
-20	0.002155	0.281374	37	–49.5	–24.64	2706	3567
-21	0.000123	0.281975	36	–28.2	–1.68	1757	2128
-22	0.001144	0.282103	36	–23.7	2.04	1626	1891
-23	0.000638	0.281953	36	–29.0	–2.90	1811	2205
-24	0.001699	0.282050	35	–25.5	–0.30	1725	2040
-25	0.001838	0.282176	32	–21.1	4.08	1552	1761
-26	0.001108	0.282127	34	–22.8	2.90	1591	1836
-27	0.001206	0.282181	42	–20.9	4.74	1520	1718
-28	0.001001	0.282018	35	–26.7	–0.89	1739	2077
-29	0.000836	0.282121	30	–23.0	2.90	1588	1836
-30	0.000722	0.281983	35	–27.9	–1.89	1774	2141
-31	0.000414	0.281570	32	–42.5	–16.28	2320	3047
-32	0.000719	0.281664	30	–39.2	–13.21	2211	2855
-33	0.001497	0.282039	32	–25.9	–0.51	1731	2054
-34	0.001122	0.281959	24	–28.8	–3.07	1826	2216
-35	0.000296	0.281561	34	–42.8	–16.51	2326	3062
-36	0.001051	0.282168	45	–21.4	4.40	1532	1741
-37	0.000536	0.282045	31	–25.7	0.47	1679	1991
-38	0.000792	0.282111	32	–23.4	2.61	1599	1854
-39	0.001210	0.282217	37	–19.6	6.02	1469	1636
-40	0.001000	0.281966	35	–28.5	–2.72	1810	2194
-41	0.000617	0.281648	30	–39.8	–13.69	2227	2885

and 0.8 Ga to 0.7 Ga. In particular the early Neoproterozoic magmatic activities around 0.8 Ga to 0.7 Ga are considered to be indicative of the South China affinity.

The age distribution of detrital zircon grains from the Penglai Group (Fig. 5) clearly demonstrates that most zircon grains crystallized between 1.8 and 1.1 Ga with age peaks at 1.7–1.6 Ga and 1.2 Ga. This feature of detrital zircon ages implies that sedimentary sources originated from terranes characterized by widespread early and late Mesoproterozoic magmatism and/or metamorphism. Magmatic activities between 1.8 and 1.6 Ga are known from the North China block (e.g., Peng *et al*., 2005 and references therein). Petrogenetically, these magmatic events were tightly related to rift tectonics and dominantly produced small-volume mafic and ultramafic dykes or dyke swarm within the North China block (Peng *et al*., 2005), which contain less and tiny zircon mineral grains. Therefore, it is reasonable to exclude the possibility that these mafic dykes contributed to the source of early Mesoproterozoic zircon grains for the Penglai Group. Although along the marginal regions of the North China block, early Mesoproterozoic magmatism can be traced (e.g., Li and Mu, 1999; Peng *et al*., 2005), which was particularly intensive in the Xiong'er area (e.g., Zhao *et al*., 2002, 2004), the absence of detrital Archean zircon

Table 4. (continued)

Analytical spot	$^{176}Lu/^{177}Hf$	$^{176}Hf/^{177}Hf$	Error 2σ	$\varepsilon_{Hf}(0)$	$\varepsilon_{Hf}(t)$ 1.2 Ga	$T_{DM}(Hf)$ (Ma)	$T_{DM}(Hf)_C$ (Ma)
PL10-1	0.001227	0.281800	14	–34.4	–8.78	2052	2577
-2	0.001874	0.281996	12	–27.4	–2.35	1810	2171
-3	0.000767	0.282087	23	–24.2	1.75	1632	1909
-4	0.000562	0.282101	28	–23.7	2.43	1604	1866
-5	0.000727	0.281980	16	–28.0	–2.00	1778	2148
-6	0.000825	0.281621	27	–40.7	–14.80	2275	2955
-7	0.000269	0.281587	28	–41.9	–15.55	2289	3002
-8	0.001186	0.282008	17	–27.0	–1.36	1760	2107
-9	0.000875	0.281526	15	–44.0	–18.20	2408	3167
-10	0.000638	0.281930	14	–29.8	–3.68	1842	2255
-11	0.001187	0.281961	12	–28.7	–3.04	1826	2214
-12	0.000548	0.281352	28	–50.2	–24.13	2624	3535
-13	0.000468	0.282143	14	–22.2	4.00	1542	1766
-14	0.000489	0.282062	16	–25.1	1.11	1654	1950
-15	0.000838	0.281982	15	–28.0	–2.03	1781	2150
-16	0.001112	0.280961	29	–64.0	–38.44	3195	4413
-17	0.000614	0.281414	31	–48.0	–21.99	2545	3403
-18	0.000584	0.281961	28	–28.7	–2.57	1798	2184
-19	0.000699	0.281926	29	–29.9	–3.88	1850	2267
-20	0.000849	0.281571	15	–42.5	–16.61	2346	3068
-21	0.000778	0.282027	29	–26.4	–0.38	1716	2045
-22	0.000887	0.282093	32	–24.0	1.89	1628	1900
-23	0.001056	0.281983	37	–27.9	–2.16	1789	2159
-24	0.000551	0.282073	33	–24.7	1.43	1642	1930
-25	0.000434	0.281834	16	–33.2	–6.95	1964	2462
-26	0.000549	0.281433	32	–47.3	–21.24	2514	3356
-27	0.001111	0.281991	45	–27.6	–1.92	1781	2143
-28	0.000427	0.281389	40	–48.9	–22.71	2566	3447
PL14-1	0.001435	0.282175	17	–21.1	4.34	1537	1744
-2	0.000840	0.281936	16	–29.6	–3.66	1844	2254
-3	0.001569	0.282270	28	–17.8	7.60	1408	1535
-4	0.001394	0.281932	13	–29.7	–4.24	1877	2290
-5	0.000399	0.282024	14	–26.5	–0.18	1703	2033
-6	0.001212	0.282153	14	–21.9	3.76	1558	1781
-7	0.001524	0.282088	17	–24.2	1.18	1664	1946
-8	0.000870	0.281606	14	–41.2	–15.37	2299	2991
-9	0.000795	0.281953	14	–29.0	–3.01	1818	2212
-10	0.000351	0.281197	14	–55.7	–29.45	2818	3863
-11	0.001178	0.282060	14	–25.2	0.49	1687	1990
-12	0.000413	0.281287	15	–52.5	–26.32	2702	3670
-13	0.001022	0.282078	39	–24.5	1.25	1655	1942
-14	0.000345	0.281576	17	–42.3	–16.02	2308	3031
-15	0.000711	0.281993	15	–27.6	–1.53	1759	2118
-16	0.000942	0.281661	16	–39.3	–13.49	2228	2873
-17	0.001149	0.282083	18	–24.4	1.33	1653	1936
-18	0.001659	0.281966	18	–28.5	–3.26	1843	2228
-19	0.001018	0.281851	21	–32.6	–6.79	1970	2452
-20	0.000817	0.281991	24	–27.6	–1.70	1767	2129
-21	0.001499	0.281168	21	–56.7	–31.40	2943	3983
-22	0.000830	0.281049	41	–60.9	–35.10	3053	4209
-23	0.000691	0.282104	31	–23.6	2.44	1605	1866
-24	0.000785	0.281936	21	–29.6	–3.61	1842	2251
-25	0.000761	0.281765	19	–35.6	–9.63	2074	2630
-26	0.000688	0.281680	16	–38.6	–12.60	2187	2817
-27	0.000782	0.281862	14	–32.2	–6.21	1942	2415
-28	0.000840	0.281636	16	–40.2	–14.30	2257	2924
-29	0.000538	0.282155	16	–21.8	4.37	1528	1742

grains in the Penglai sedimentary rocks implies that the Archean basements of the North China block did not provide sedimentary material during the sedimentation of the Penglai Group. Recent geochronological studies have shown that early Mesoproterozoic zircons can be found also in the Yangtze block (e.g., Zheng *et al*., 2006) and in the Cathaysia block (Wang, Y.-S., private communication). Contrarily, the basements of the Yangtze block are characterized by Mesoproterozoic and Neoproterozoic thermotectonic events, especially between 1.3 and 1.0 Ga (related to the Grenville orogeny) and between 0.8 and 0.7 Ga (related to the breakup of Rodinia). Temporally, the Grenville event corresponds to the Sibao orogeny in Chinese literature. This event is widely traced in the Yangtze and Cathaysia blocks that finally collided around 1.0 Ga forming the South China block (e.g., Ma and Bai, 1998; Li *et al*., 1994, 2002; Li, 1996; Chen *et al*., 1991; Shui, 1987; Li and Mu, 1999). In this context, it is reasonable to consider the Yangtze (and Cathaysia) block(s) as the major source for the sedimentary material. We therefore suggest that the Penglai Group, probably together with the Fenzishan Group (Tang *et al*., 2006), is of the Yangtze affinity and was thrust onto the Archean-Paleoproterozoic basements of the North China block during the Mesozoic continental collision that led to the formation of the Dabie-Sulu UHP orogenic belt. This interpretation can be supported by the crustal-detachment model for tectonic architecture of the Dabie-Sulu orogenic belt (Li, 1994, 1998), in which the Sulu terrane is considered to represent an upper part of the South China (Yangtze) block displaced northwards by the Tanlu fault after the collision between the North and South China blocks. In this context, the boundary between the South and North China blocks in the Sulu area can be located further north as suggested by Faure *et al*. (2001).

Sedimentation time

Detrital zircon grains from low-grade sedimentary rocks crystallized before the erosion of their host rocks, i.e., before transport and deposition of the eroded material. Therefore, ages of the youngest detrital zircon grains can be used to constrain the upper limit of the deposition time. The sedimentary rocks of the Penglai Group contain zircons as young as 1.1 Ga, which mark an upper limit for the deposition time. As mentioned above, late Proterozoic magmatic activity (~0.8–0.7 Ga) is widely distributed within the South China block, especially in the Yangtze block (e.g., Li *et al*., 2003; Zheng *et al*., 2005; Chen, F. *et al*., 2003). As late Proterozoic detrital zircon grains are absent from the Penglai Group, it is reasonable to suggest a lower age limit of 0.8 Ga for the deposition time of the Penglai sedimentary rocks. These constraints on the deposition time are significantly different from those Paleozoic ages obtained by the Rb-Sr and paleontological dating reported previously (Zhu *et al*., 1994; Ji and Zhao, 1992), but similar to whole-rock Pb-Pb age of 1166 Ma (Zhang, 1995). With respect to the sedimentation time, the late Mesoproterozoic to early Neoproterozoic Penglai Group is different from the low-grade Paleozoic Foziling Group and the Neoproterozoic to Paleozoic (?) Luzhenguan Group along the northern margin of the Dabie UHP terrane (Chen, F. *et al*., 2003) and from the low-grade Neoproterozoic Wulian Group in the Sulu UHP terrane (Zhou *et al*., 2001, 2003, 2005).

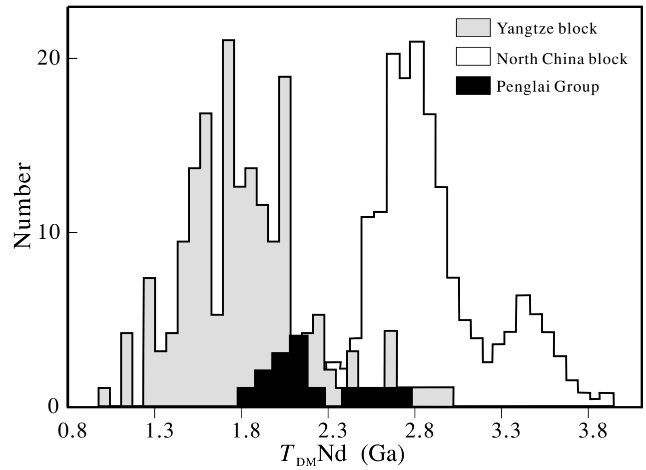

Fig. 7. Frequency histogram of T_{DM}(Nd) values of whole-rock samples compared to basement rocks from the Yangtze and North China blocks. Model Data of these two blocks compiled in Chen and Jahn (1998) and Wu et al. (2005). One-stage model ages are used for plot.

Nd-Hf isotopic constraints on sedimentary sources

Nd isotopic composition of sedimentary rocks can provide useful information about the formation and evolution of the continental crust, owing to the relatively immobile characteristic of the Sm-Nd isotopic system (e.g., Liew and Hofmann, 1988). Initial $^{143}Nd/^{144}Nd$ isotopic ratios (ε_{Nd}) and depleted-mantle model ages (T_{DM}) characterize the source of sedimentary rocks and therefore have been widely applied for studies on tectonic evolution of continental blocks. The model ages obtained by whole-rock analyses are commonly interpreted as average crustal formation ages of the sedimentary source(s).

The North China block is interpreted as an assemblage of old basement rocks that were mainly formed and accreted during the Archean and came together around 1.9 Ga to 1.8 Ga (e.g., Zhao, 2001), while the major basement rocks of the Yangtze block formed during the Paleo- to Mesoproterozoic period (e.g., Yang *et al*., 1986; Ma and Bai, 1998; Lu, 1998; Zhai *et al*., 2000; Zhao, 2001). Statistics of the T_{DM}(Nd) values from both continental blocks (Fig. 7), compiled by Wu *et al*. (2005), show that the North China block has had two major crustal formation periods at about 3.4 and 2.8 Ga. Except for small outcrops of Archean rocks along the northern and northwestern margins (e.g., Gao *et al*., 2001), basements of the Yangtze block mainly formed during the Paleo- to Mesoproterozoic. Distribution of the T_{DM}(Nd) values of sedimentary rocks from the Yangtze block suggests a time period of about 2.0 Ga for formation of the major crustal edifices within this cratonic block (Wu *et al*., 2005; Chen and Jahn, 1998). T_{DM}(Nd) values of sedimentary rocks from the Penglai Group range from 2.8 Ga to 1.8 Ga with a peak at 2.2–2.0 Ga, indicating a Paleoproterozoic mean crustal residence time for the sources of the Penglai Group. Comparison of the distribution of T_{DM}(Nd) values for the Penglai Group (Fig. 7), with that of the Yangtze block and the North China block (Wu *et al*., 2005; Chen and Jahn, 1998; and references therein), indicates that the crustal residence time distribution of the sedimentary sources for the Penglai Group is more akin to the distribution found within the Yangtze block. Initial ε_{Nd} values of the Penglai Group, calculated back to 1.2 Ga (Table 2), range from –6.4 to –1.7, also distinguishably higher than those of the basement rocks from the North China block, when compared at 1.2 Ga (data compiled by Wu *et al*., 2005).

The zircon Lu-Hf isotopic system is commonly accepted to have a very high isotopic closure temperature such that Hf isotopic composition of zircon can preserve source information, even for high-grade metamorphic rocks, such as granulites (Scherer *et al*., 2000). Therefore, compared to whole-rock Sm-Nd data, we believe that Hf isotopic composition of detrital zircon grains, obtained by the LA-MC-ICP MS *in-situ* method, can be more suitable for offering information about the source characteristics of sedimentary rocks. Distribution of zircon T_{DM}(Hf) values (Fig. 6), calculated using a mean crustal Lu/Hf ratio (^{176}Lu/^{177}Hf ratio of 0.015; Veevers *et al*., 2005), implies complex sedimentary sources as indicated by variant T_{DM}(Hf) values ranging from about 4.0 to 1.5 Ga. Nevertheless, a peak T_{DM}(Hf) value of about 2.4 Ga to 1.5 Ga indicates that sedimentary material originated mainly from sources formed during Paleo- to Mesoproterozoic times, which are highly similar to the Yangtze block. Those zircon grains having Archean T_{DM}(Hf) values can be provided either by the North China or the Yangtze block because small Archean basement blocks, such as the Archean Kongling Complex (Fig. 1), are also exposed along the northern margin of the Yangtze block (e.g., Gao *et al*., 2001). Further comparison of zircon Hf isotopic compositions needs solid data sets from both continental blocks.

In summary, evidence from Nd-Hf isotopic composition probably supports that crustal terranes, Paleo- to Mesoproterozoic in age, provided major sedimentary material for the Penglai Group. This characteristic closely correlates with the main crustal formation periods within the Yangtze block, but clearly differs from that of the North China block. Therefore, an affinity of the South China block (especially the Yangtze block) is implied for the Penglai Group.

CONCLUSIONS

Detrital zircon grains from low-grade sedimentary rocks of the Penglai Group are characterized by Mesoproterozoic crystallization ages, clustering at 1.7–1.6 Ga and around 1.2 Ga. This age information indicates that the products of widespread Mesoproterozoic magmatism in the South China block were the dominant sources of the sediments. The 1.2 Ga zircon grains can be taken as evidence that the sedimentary material derived from the boundary between the Yangtze and the Cathaysia block that was formed by plate convergence during late Mesoproterozoic.

Evidence from Nd isotopic composition indicates that the sediments of the Penglai Group were derived from Paleo- to Mesoproterozoic source rocks similar to average crustal material of the Yangtze block. This identity implies that the low-grade Penglai Group, situated north to the Sulu UHP terrane, originated from the South China block and not from the North China block. Absence of Neoproterozoic detrital zircon grains from the Penglai sediments probably suggests a deposition age of about 1.1 to 0.8 Ga for the Penglai Group.

Acknowledgments—This study was supported by the National Natural Science Foundation of China (NSFC project Nos. 40525007 and 40421202) and by the Ministry of Science and Technology of China (G1999075502). Z.-X. Li, T. Komiya and K. Yamashita are gratefully acknowledged for constructive comments and helpful suggestions to improve the manuscript. Sincere thanks are due to J.-H. Yang for help in zircon Hf isotopic measurement and discussion.

REFERENCES

Ames, L., Tilton, G. R. and Zhou, G. (1993) Timing of collision of the Sino-Korean and Yangtze Cratons: U-Pb zircon dating of coesite-bearing eclogites. *Geology* **21**, 339–342.

Ames, L., Zhou, G.-Z. and Xiong, B.-C. (1996) Geochronology and isotopic character of ultrahigh pressure metamorphism with implications for collision of the Sino-Korean and Yangtze cartons, central China. *Tectonics* **15**, 472–489.

Banno, S., Enami, M., Hirajima, T., Ishiwatari, A. and Wang, Q.-C. (2000) Decompression P-T path of coesite eclogite to granulite from Weihai, eastern China. *Lithos* **52**, 97–108.

Blichert-Toft, J. and Albarede, F. (1998) The Lu-Hf geochemistry of chondrites and evolution of the mantle-crust system. *Earth Planet. Sci. Lett.* **148**, 243–258.

Chen, F., Hegner, E. and Todt, W. (2000) Zircon ages, Nd isotopic and chemical compositions of orthogneisses from the Black Forest, Germany—evidence for a Cambrian magmatic arc. *Int. J. Earth Sci.* **88**, 791–802.

Chen, F., Siebel, W. and Satir, M. (2002) Zircon U-Pb and Pb-isotope fractionation during stepwise HF-acid leaching and geochronological implications. *Chem. Geol.* **191**, 153–162.

Chen, F., Guo, J.-H., Jiang, L.-L., Siebel, W., Cong, B.-L. and Satir, M. (2003) Provenance of the Beihuaiyang lower-grade metamorphic zone of the Dabie ultrahigh-pressure collisional orogen, China: evidence from zircon ages. *J. Asian Earth Sci.* **22**, 343–352.

Chen, F., Li, Q.-L., Li, C.-F., Li, X.-H., Wang, X.-L. and Wang, F. (2005) Prospect of high precision mass spectrometer in isotope Geochemistry. *Earth Sci.* **30**, 639–645 (in Chinese with English abstract).

Chen, F., Li, X.-H., Wang, X.-L., Li, Q.-L. and Siebel, W. (2006) Nd-Hf isotopic composition and basement age of the Baoshan block in the Yunnan Tethyan belt, SW China: evidence from Early Paleozoic and Early Mesozoic granites. *Int. J. Earth Sci.* (submitted).

Chen, J. and Jahn, B. (1998) Crustal evolution of southeastern China: Nd and Sr isotopic evidence. *Tectonophysics* **284**, 101–133.

Chen, J., Foland, K. A., Xing, F., Xu, X. and Zhou, T. (1991) Magmatism along the southeast margin of the Yangtze block: Precambrian collision of the Yangtze and Cathaysia block of China. *Geology* **19**, 815–818.

Chen, J.-F., Xie, Z., Li, X.-D., Zhang, T.-X., Zhou, Y.-S., Park, K. S., Ahn, K. S., Chen, D.-G. and Zhang, X. (2003) U-Pb zircon ages for a collision-related K-rich complex at Shidao in the Sulu ultrahigh pressure terrane, China. *Geoch. J.* **37**, 35–46.

Chu, N. C., Taylor, R. N., Chavagnac, V., Nesbitt, R. W., Boella, R. M., Milton, J. A., German, C., Bayon, G. and Burton, M. (2002) Hf isotope ratio analysis using multi-collector inductively coupled plasma mass spectrometry: an evaluation of isobaric interference corrections. *J. Anal. At. Spectrom.* **17**, 1567–1574.

Cong, B.-L. (1996) *Ultrahigh-pressure Metamorphic Rocks in the Dabie-Sulu Region of China*. Science Press, Beijing, China and Kluwer Academic Publishing, Dordrecht, 224 pp.

DePaolo, D. J., Linn, A. M. and Schubert, G. (1991) The continental crustal age distribution; methods of determining mantle separation ages from Sm-Nd isotopic data and application to the Southwestern United States. *J. Geophys. Res.* **96B**, 2071–2088.

Faure, M., Lin, W. and Breton, N. L. (2001) Where is the North China-South China block boundary in eastern China? *Geology* **29**, 119–122.

Gao, S., Qiu, Y., Ling, W., McNaughton, N. J. and Groves, D. I. (2001) Single zircon SHRIMP U-Pb geochronology of the Kongling high-grade metamorphic terrain—A discovery of >3.2 Ga crustal material in the Yangtze craton. *Sci. in China (D)* **31**, 27–35 (in Chinese).

Griffin, W. L., Pearson, N. J., Belousova, E., Jackson, S. E., van Achterbergh, E., O'Reilly, S. Y. and Shee, S. R. (2000) The Hf isotope composition of cratonic mantle: LAM-MC-ICPMS analysis of zircon megacrysts in kimberlites. *Geochim. Cosmochim. Acta* **64**, 133–147.

Gromet, L. P., Dymek, R. F., Haskin, L. A. and Korotev, R. L. (1984) The "North Ameican Shale Composite": its compilation, major and trace element characteristics. *Geochim. Cosmochim. Acta* **48**, 2469–2482.

Guo, J.-H., Chen, F., Zhang, X.-M., Siebel, W. and Zhai, M.-G. (2005) Evolution of syn- to post-collisional magmatism from north Sulu UHP belt, eastern China: zircon U-Pb geochronology. *Acta Petrol. Sinica* **21**, 1281–1301 (in Chinese with English abstract).

Hacker, B. R., Ratschbacher, L., Webb, L., Ireland, T., Walker, D. and Dong, S. (1998) U/Pb zircon ages constrain the architecture of the ultrahigh-pressure Qinling-Dabie orogen, China. *Earth Planet. Sci. Lett.* **161**, 215–230.

Hanchar, J. M. and Miller, C. F. (1993) Zircon zonation patterns as revealed by cathodoluminescence and backscattered electron images: Implications for interpretation of complex crustal histories. *Chem. Geol.* **110**, 1–13.

Hoskin, P. W. O. and Black, L. P. (2000) Metamorphic zircon formation by solid-state recrystallization of potolith igneous zircon. *J. Metamorphic Geol.* **18**, 423–439.

Hsü, K. J., Wang, Q., Li, J., Zhou, D. and Sun, S. (1987) Tectonic evolution of Qinling Mountains, China. *Eclog. Geol. Helv.* **80**, 735–752.

Iizuka, T., Hirata, T., Komiya, T., Rino, S., Katayama, I., Motoki, A. and Maruyama, S. (2005) U-Pb and Lu-Hf isotope systematics of zircons from the Mississippi River sand: implications for reworking and growth of continental crust. *Geology* **33**, 485–488.

Ishizaka, K., Hirajima, T. and Zheng, X.-S. (1994) Rb-Sr dating for the Jiaodong gneiss of the Su-Lu ultra-high pressure province, eastern China. *Island Arc* **3**, 232–241.

Jahn, B.-M., Cornichet, J., Cong, B.-L. and Yui, T.-F. (1996) Ultrahigh ε_{Nd} eclogites from an ultrahigh-pressure metamorphic terrane of China. *Chem. Geol.* **127**, 61–79.

Ji, Z.-Y. and Zhao, H.-J. (1992) New evidence for age of the Penglai Group in eastern Shandong. *J. Stratigraphy* **16**, 237–238 (in Chinese).

Kober, B. (1986) Whole-grain evaporation for $^{207}Pb/^{206}Pb$-age-investigations on single zircons using a double-filament thermal ion source. *Contrib. Mineral. Petrol.* **93**, 482–490.

Kober, B. (1987) Single-Zircon evaporation combined with Pb^+ emitter bedding for $^{207}Pb/^{206}Pb$-age investigations using thermal ion mass spectrometry, and implications to zirconology. *Contrib. Mineral. Petrol.* **96**, 63–71.

Li, J.-H. and Mu, J. (1999) Tectonic constraints from Chinese cratonic blocks for the reconstruction of Rodinia. *Scientia Geol. Sinica* **34**, 259–272 (in Chinese with English abstract).

Li, S.-G., Xiao, Y.-L., Liou, D.-L., Chen, Y.-Z., Ge, N.-J., Zhang, Z.-Q., Sun, S.-S., Cong, B.-L., Zhang, R.-Y., Hart, S. R. and Wang, S.-S. (1993) Collision of the North China and Yangtze Blocks and formation of coesite-bearing eclogites: Timing and processes. *Chem. Geol.* **109**, 89–111.

Li, S.-G., Jagoutz, E., Lo, C.-H., Chen, Y.-Z. and Li, Q.-L. (1999) Sm/Nd, Rb/Sr and $^{40}Ar/^{39}Ar$ isotopic systematics of the ultrahigh-pressure metamorphic rocks in the Dabie-Sulu belt central China: a retrospective view. *Int. Geol. Rev.* **41**, 1114–1124.

Li, X.-H. (1996) Sm-Nd isotopic systematics of Sibao Group from the southern margin of Yangtze block: implications for the crustal evolution. *Scientia Geolog. Sinica* **31**, 218–228 (in Chinese with English abstract).

Li, X.-H., Zhou, G., Zhao, J., Fanning, C. M. F. and Compston, W. (1994) SHRIMP ion microprobe zircon U-Pb age of the NE Jiangxi ophiolite and its tectonic implications. *Geochemica* **23**, 125–131.

Li, Z.-X. (1994) Collision between the North and South China blocks: A crustal-detachment model for suturing in the region east of the Tanlu fault. *Geology* **22**, 739–742.

Li, Z.-X. (1998) Tectonic history of the major East Asian lithospheric blocks since the Mid-Proterozoic—a synthesis. *Mantle Dynamics and Plate Interactions in East Asia* (Flower, M. F. J. *et al*., eds.), AGU Geodynamic Series **27**, 221–243.

Li, Z.-X., Li, X.-H., Zhou, H.-W. and Kinny, P. D. (2002) Grenvillen continental collision in south China: new SHRIMP U-Pb zircon results and implications for the configuration of Rodinia. *Geology* **30**, 163–166.

Li, Z.-X., Li, X.-H., Kinny, P. D., Wang J., Zhang, S. and Zhou, H. (2003) Geochronology of Neoproterozoic syn-rift magmatism in the Yangtze Craton, South China and correlations with other continents: evidence for a mantle superplume that broke up Rodinia. *Precamb. Res.* **122**, 85–109.

Liew, T. C. and Hofmann, A. W. (1988) Precambrian crustal components, plutonic associations, plate environment of the Hercynian Fold Belt of central Europe: Indications from a Nd and Sr isotopic study. *Contrib. Mineral. Petrol.* **98**, 129–138.

Liou, J. G., Zhang, R. Y., Eide, E. A., Maruyama, S., Wang, X. and Ernst, W. G. (1996) Metamorphism and tectonics of high-P and ultrahigh-P belts in Dabie-Sulu regions, eastern central China. *The Tectonic Evolution of Asia* (Yin, A. and Harrison, T. M., eds.), 300–343, Cambridge University, New York.

Liu, J.-B., Ye, K., Maruyama, S., Cong, B.-L. and Fan, H.-R. (2001) Mineral inclusions in zircon from gneisses in the ultrahigh-pressure zone of the Dabie Mountains, China. *J. Geol.* **109**, 523–535.

Lu, S.-N. (1998) A review of advance in the research on the Neoproterozoic Rodinia supercontinent. *Geol. Rev.* **44**, 489–495 (in Chinese with English abstract).

Ludwig, K. R. (2001) *Isoplot/Ex, rev 2.49: A Geochronological toolkit for Microsoft Excel*. Berkeley Geochron. Center Spec. Publ. No. 1a, 58 pp.

Ma, X.-Y. and Bai, J. (1998) *Precambrian Crustal Evolution of China*. Springer Berlin-Heidelberg, Geol. Publishing House Beijing, 331 pp.

Machado, N. and Simonetti, A. (2001) U-Pb dating and Hf isotopic composition of zircon by laser ablation MC-ICP-MS. *Laser Ablation-ICPMS in the Earth Sciences: Principles and Applications* (Sylvester, P., ed.), St. John's, Newfoundland, Mineral. Assoc. Canada **29**, 121–146.

Mattauer, M., Matte, Ph., Malavieille, J., Tapponnier, P., Maluski, H., Xu, Z., Lu, Y. and Tang, Y. (1985) Tectonics of the Qinling belt: build-up and evolution of eastern Asia. *Nature* **317**, 496–500.

Meng, Q.-R. and Zhang, G.-W. (1999) Timing of collision of the North and South China blocks: Controversy and reconciliation. *Geology* **27**, 123–126.

Meng, Q.-R. and Zhang, G.-W. (2000) Geologic framework and tectonic evolution of the Qinling orogen, central China. *Tectonophysics* **323**, 183–196.

Nelson, D. R. (2001) An assessment of the determination of depositional ages for Precambrian clastic sedimentary rocks by U-Pb dating of detrital zircons. *Sediment. Geol.* **141–142**, 37–60.

Niu, B.-X., Liu, S.-C. and Liu, H.-S. (1996) The age of the Penglai Group in Qixia region belongs to the Sinian period. *Geol. Shandong* **12**, 63–68 (in Chinese with English abstract).

Peng, P., Zhai, M.-G., Zhang, H.-F. and Guo, J.-H. (2005) Geochronological constraints on the Paleoproterozoic evolution of the North China Craton: SHRIMP zircon ages of different types of mafic dikes. *Int. Geol. Rev.* **47**, 1–17.

Pidgeon, R. T., Nemchin, A. A. and Hitchen, G. J. (1998) Internal structures of zircons from Archaean granites from the Darling Range Batholith; implications for zircon stability and the interpretation of zircon U-Pb ages. *Contrib. Mineral. Petrol.* **132**, 288–299.

Qiu, Y.-M., Gao, S., McNaughton, N. J., Groves, D. I. and Ling, W.-L. (2000) First evidence of >3.2 Ga continental crust in the Yangtze craton of south China and its implications for Archean crustal evolution and Phanerozoic tectonics. *Geology* **28**, 11–14.

Rino, S., Komiya, T., Windley, B. F., Katayama, I., Motoki, A. and Hirata, T. (2004) Major episodic increases of continental crustal growth determined from zircon ages of river sands: implications for mantle overturns in the Early Precambrian. *Phys. Earth Planet. Inter.* **146**, 369–394.

Rubatto, D. (2002) Zircon trace element geochemistry: partitioning with garnet and the link between U-Pb ages and metamorphism. *Chem. Geol.* **184**, 123–138.

Scherer, E. E., Cameron, K. L. and Blichert-Toft, J. (2000) Lu-Hf garnet geochronology: closure temperature relative to the Sm-Nd system and the effects of trace mineral inclusions. *Geochim. Cosmochim. Acta* **64**, 3413–3432.

Shui, T. (1987) Tectonic frame of the continental basement in southeastern China. *Sci. in China (B)* **13**, 414–422.

Stacey, J. S. and Kramers, J. D. (1975) Approximation of terrestrial lead isotope evolution by a two stage model. *Earth Planet. Sci. Lett.* **26**, 207–221.

Sun, S. S. (1982) Chemical composition and origin of the Earth's primitive mantle. *Geochim. Cosmochim. Acta* **46**, 179–192.

Tang, J., Zheng, Y.-F., Wu, Y.-B. and Gong, B. (2006) Zircon SHRIMP U-Pb dating, C and O isotopes for impure marbles from the Jiaobei terrane in the Sulu orogen: implication for tectonic affinity. *Precamb. Res.* **144**, 1–18.

Taylor, S. R. and McLennan, S. M. (1985) *The Continental Crust: Its Composition and Evolution*. Blackwell, Oxford, 312 pp.

Valverde, V. P., Doerr, W., Belka, Z., Franke, W., Wiszniewska, J. and Schastok, J. (2000) U-Pb single-grain dating of detrital zircon in the Cambrian of central Poland; implications for Gondwana versus Baltica provenance studies. *Earth Planet. Sci. Lett.* **184**, 225–240.

Veevers, J. J., Saeed, A., Belousova, E. A. and Griffin, W. L. (2005) U-Pb ages and source composition by Hf-isotope and trace-element analysis of detrital zircons in Permian sandstone and modern sand from southwestern Australia and a review of the paleogeographical and denudational history of the Yilgarn Craton. *Earth-Sci. Rev.* **68**, 245–279.

Wang, L.-G., Qiu, Y. M., McNaughton, N. J., Groves, D. I., Luo, Z. K., Huang, J. Z., Miao, L. C. and Liu, Y. K. (1998) Constraints on crustal evolution and gold metallogeny in the Northwestern Jiaodong Peninsula, China, from SHRIMP U-Pb zircon studies of granitoids. *Ore Geol. Rev.* **13**, 275–291.

Wang, Q.-C., Ishiwatari, A., Zhao, Z.-Y., Hirajima, T., Hiramatsu, N., Enami, M., Zhai, M.-G., Li, J.-J. and Cong, B.-L. (1993) Coesite bearing granulite retrograded from eclogite in Weihai, eastern China. *Eur. J. Mineral.* **5**, 141–152.

Wang, X., Liou, J. G. and Mao, H.-K. (1989) Coesite-bearing eclogites from the Dabie Mountains in Central China. *Geology* **17**, 1085–1088.

Wiedenbeck, M., Allé, P., Corfu, F., Griffin, W. L., Meier, M., Oberli, F., von Quadt, A., Roddick, J. C. and Spiegel, W. (1995) Three natural zircon standards for U-Th-Pb, Lu-Hf, trace element and REE analyses. *Geostand. Newslett.* **19**, 1–23.

Woodhead, J., Hergt, J., Shelley M., Eggins, S. and Kemp, R. (2004) Zircon Hf-isotope analysis with an excimer laser, depth profiling, ablation of complex geometries, and concomitant age estimation. *Chem. Geol.* **209**, 121–135.

Wu, F.-Y., Zhao, G.-C., Wilde, S. A. and Sun, D.-Y. (2005) Nd isotopic constraints on crustal formation in the North China Craton. *J. Asian Earth Sci.* **24**, 523–545.

Wu, Y.-B., Zheng, Y.-F., Gong, B., Tang, J., Zhao, Z.-F. and Zha, X.-P. (2004) Zircon U-Pb ages and oxygen isotope compositions of the Luzhenguan magmatic complex in the Beihuaiyang zone. *Acta Petrolog. Sinica* **20**, 1007–1024 (in Chinese with English abstract).

Xu, P., Wu, F.-Y, Xie, L.-W. and Yang, J.-H. (2004) Hf isotopic compositions of the standard zircons for U-Pb dating. *Chinese Sci. Bull.* **49**, 1642–1648.

Xu, S.-T., Okay, A. I., Sengor, A. M. C., Su, W., Liu, Y. and Jiang, L. (1992) Diamond from Dabie Shan eclogites and its implication for tectonic setting. *Science* **256**, 80–82.

Yang, J.-H., Chung, S. L., Wilde, S. A., Wu, F.-Y., Chu, M. F., Lo, C. H. and Fan, H.-R. (2005) Petrogenesis of post-orogenic syenites in the Sulu orogenic belt, East China: geochronological, geochemical and Nd-Sr isotopic evidence. *Chem. Geol.* **214**, 99–125.

Yang, Z.-Y., Cheng, Y.-Q. and Wang, H.-Z. (1986) *The Geology of China*. Oxford Monographs Geol. Geophys. 3, Oxford, 303 pp.

Yin, A. and Nie, S. (1993) An indentation model for the North and South China collision and the development of the Tan-Lu and Honam fault systems, eastern Asia. *Tectonics* **12**, 801–813.

Zhai, M., Cong, B., Guo, J., Liu, W., Li, Y. and Wang, Q. (2000) Sm-Nd geochronology and petrography of garnet pyroxene granulites in the northern Sulu region of China and their geotectonic implication. *Lithos* **52**, 23–33.

Zhang, G.-W., Meng, Q. and Lai, S. (1995) Tectonics and structures of the Qinling orogenic belt. *Sci. in China (D)* **38**, 1379–1386.

Zhang, R.-Y., Hirajima, T., Banno, S., Cong, B.-L. and Liou, J. G. (1995) Petrology of ultrahigh pressure rocks from the southern Sulu region, eastern China. *J. Metamorphic Geol.* **13**, 659–675.

Zhang, W.-Q. (1995) Discussion on lead isotope compositions of the Fenzishan and Penglai Groups in the Jiaodong region. *Shandong Geol.* **11**, 18–24 (in Chinese with English abstract).

Zhao, G.-C. (2001) Palaeoproterozoic assembly of the North China Craton. *Geol. Mag.* **138**, 87–91.

Zhao, G.-C. and Cawood, P. A. (1999) Tectonothemal evolution of the Mayuan assemblage in the Cathaysia block: implications for Neoproterozoic collision-related assembly of the South China Craton. *Am. J. Sci.* **299**, 309–339.

Zhao, T.-P., Zhou, M.-F., Zhai, M.-G. and Xia, B. (2002) Palaeoproterozoic rift-related volcanism of the Xiong'er Group in the North China Craton: implications for the break-up of Columbia. *Int. Geol. Rev.* **44**, 336–351.

Zhao, T.-P., Zhai, M.-G., Xia, B., Li, H.-M. and Zhang, Y.-X. (2004) Study on the zircon SHRIMP ags of the Xiong'er Group volcanic rocks: constraint on the starting time of covering strata in the North China Craton. *Chinese Sci. Bull.* **9**, 2495–2502.

Zheng, J.-P., Griffin W. L., O'Reilly, S. Y., Zhang, M., Pearson, N. and Pan, Y.-M. (2006) Widespread Archean basement beneath the Yangtze craton. *Geology* **34**, 417–420.

Zheng, Y.-F., Wang, Z.-R., Li, S.-G. and Zhao, Z.-F. (2002) Oxygen isotope equilibrium between eclogite minerals and its constraints on mineral Sm-Nd chronometer. *Geochim. Cosmochim. Acta* **66**, 625–634.

Zheng, Y.-F., Zhou, J.-B., Wu, Y.-B. and Xie, Z. (2005) Low-grade metamorphic rocks in the Dabie-Sulu orogenic belt: A passive-margin accretionary wedge deformed during continent subduction. *Int. Geol. Rev.* **47**, 851–871.

Zhou, J.-B., Zheng, Y.-F., Li, L. and Xie, Z. (2001) On low-grade metamorphic rock within Dabie-Sulu ultrahigh pressure metamorphic belt. *Acta Petrol. Sinica* **17**, 39–48 (in Chinese with English abstract).

Zhou, J.-B., Zheng, Y.-F. and Wu, Y.-B. (2003) Zircon U-Pb ages for Wulian granites in northern Sulu and their tectonic implications. *Chinese Sci. Bull.* **48**, 379–384.

Zhou, J.-B., Liu, J.-H. and Zheng, C.-Q. (2005) Geological genesis and tectonic implications of low-grade metamorphic rocks in Sulu orogenic belt. *Acta Geolog. Sinica* **79**, 475–486 (in Chinese with English abstract).

Zhu, G., Xu, J.-W., Fitches, W. R. and Fletcher C. J. N. (1994) Isotopic ages of the Penglai Group in the Jiaobei belt and their geotectonic implications. *Acta Geolog. Sinica* **68**, 158–172 (in Chinese with English abstract).